Snap-Back Analysis of Fracture Evolution in Multi-cracked Masonry Arches

Renato Cafarelli[1(✉)], Federico Accornero[2], and Alberto Carpinteri[1,2]

[1] Politecnico di Torino, Turin, Italy
renato.cafarelli@polito.it
[2] Shantou University, Shantou, People's Republic of China

Abstract. In the present work, the Cohesive/Overlapping Crack Model is extended to the study of masonry or plain concrete structures, which are subjected to off-center compression. Multi-cracking and multi-crushing damage phenomena are simulated by means of the Crack Length Control Scheme, in order to obtain a complete load history of the vaulted structure. This Nonlinear Fracture Mechanics model reveals a high capability in predicting the elastic-plastic-softening behaviour of arches and vaults as well as the local mechanical instabilities, such as snap-back and snap-through, occurring during the post-cracking regime.

In the first part of this paper, the Cohesive/Overlapping Crack Model and a description of the adopted multi-crack numerical procedures is provided. In the second part, some parametric analyses on scale effects in masonry arches are reported together with the results obtained for a real case-study. Finally, some future developments and applications of the model are presented.

Keywords: Cracking · Crushing · Scale effects · Cohesive Crack Model · Overlapping Crack Model

1 Introduction

1.1 Structural Theories for Masonry Arches

The design of masonry arch bridges during 19th and 20th centuries was based on Theory of Elasticity: the shape of the arch was chosen as close as possible to the line of thrust of the loads acting on the structure in order to reduce the tensile stresses generated by bending moment [1–3]. This design approach leads to the construction of very massive structures in which the variation of the thrust line due to live loads is negligible with respect to the position of the thrust line generated by dead loads [4, 5].

On the other hand, with the extension of Theory of Plasticity to masonry structures due to Heyman [6], it was provided that a limit condition is reached when the thrust line is tangent to the structure cross-section: in this case, a plastic hinge is formed and a variation in the internal stresses is obtained. The design of masonry arches by means of this approach leads to lighter structures as well as to material optimization since the thrust line is no longer forced to pass through the central kern of the cross-section [1, 7].

S. Gabriele et al. (Eds.): IWSS 2023, LNCE 437, pp. 80–87, 2024.
https://doi.org/10.1007/978-3-031-44328-2_9

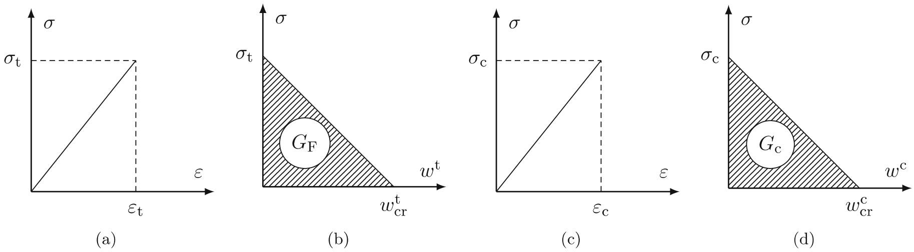

Fig. 1. Cohesive and Overlapping Crack Models: (a) Linear elastic stress – strain law in tension; (b) Post-peak σ-w^{t} cohesive relationship; (c) Linear elastic stress – strain law in compression; (d) Post-peak stress vs fictitious interpenetration relationship

In this context, although the two fundamental theorems of Theory of Plasticity may be used to define the limit condition and the loadbearing capacity of a structure, they are not able to clarify how this condition is reached. On the other hand, recent applications [1, 8] of Linear Elastic Fracture Mechanics (LEFM) have demonstrated that an increase in the bearing capacity of a masonry arch may be obtained by means of an increase in the cracking damage: due to cracking, a recentering of the thrust line is obtained and a fracturing benefit coefficient may be defined.

In the present paper, an extension of the Cohesive/Overlapping Crack Model (COCM) [9–15] is presented. This model is able to evaluate the elastic-plastic-softening loading history of masonry structures taking into account the damage evolution in tension as well as in compression together with scale effects.

1.2 The Cohesive/Overlapping Crack Model

COCM is a Nonlinear Fracture Mechanics model that integrates the Cohesive Crack Model to simulate the damaging process occurring in tension with the Overlapping Crack Model to simulate the damaging process occurring in compression. The Cohesive Crack Model [16, 17] is able to describe the damage evolution in the tension zone of a structure, assuming a linear elastic constitutive law (Fig. 1a) up to the first peak load, and a constitutive law in the form σ-w^{t}, σ being the applied stress and w^{t} the crack opening displacement, in the zone where strain localization in tension occurs [17]. More precisely, within the Cohesive Crack Model, a fictitious crack, longer than the real one, is introduced, providing a damage process zone where the material is still able to transfer tensile forces, albeit partially damaged. Thus, the residual bearing capacity of the structural element is simulated by means of the application of closing forces along the crack faces according to the constitutive law of Fig. 1b, where $w^{t}{}_{cr}$ is the threshold value of crack opening beyond which the closing forces vanish. The area subtended by the σ-w^{t} diagram represents the fracture energy, G_F (see Fig. 1b).

The Cohesive Crack Model has been effectively applied in the study of plain concrete or lightly reinforced/high strength concrete beams as well as in the nonlinear behaviour of masonry structures, not considering the potential crushing failure occurring in compression zones [18, 19]. In this framework, Carpinteri and co-workers [20] introduced

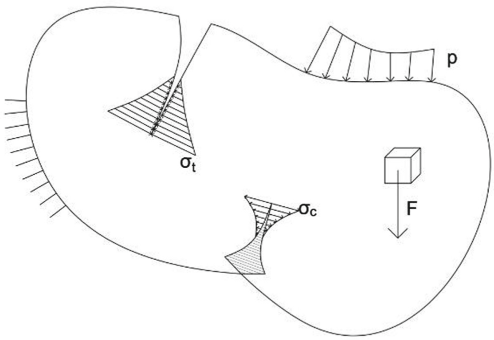

Fig. 2. Damaged body with process zones in tension and compression

the Overlapping Crack Model, which is able to describe the crushing damage of a quasi-brittle material by means of a fictitious interpenetration zone developing in the region where compressive strain localization takes place. The parameters involved in the Overlapping Crack Model are formally similar to those of the Cohesive Crack Model. The main variables entailed within this model are: the compressive strength of the material, σ_c, the threshold value of fictitious interpenetration beyond which the virtual opening compressive forces vanish, $w^c{}_{cr}$, and the crushing energy, G_c, which may be calculated as the area subtended by the σ-w^c diagram of Fig. 1d. Within the Overlapping Crack Model, the material behaves elastically until the compression strength σ_c is reached (Fig. 1c), then a constitutive law in the form σ-w^c (Fig. 1d) is adopted.

2 Numerical Algorithm

COCM may be integrated in a finite element method. In this context, for an undamaged elastic solid body, the weak form of equilibrium [21] leads to

$$\int_V \delta\{\varepsilon\}^T\{\sigma\}dV = \int_V \delta\{u\}^T\{F\}dV + \int_S \delta\{u\}^T\{t\}dS \tag{1}$$

$\{F\}$ being the vector of the forces acting on the volume of the body, $\{t\}$ the vector of the forces acting on the surface of the body, $\{u\}$ the displacement vector, and S the body surface. On the other hand, for a damaged solid having m cohesive cracks and n overlapping process zones (Fig. 2), the last term of Eq. (1) may be decomposed as

$$\begin{aligned}\int_S \delta\{u\}^T\{t\}dS = \sum_j^m \left(\int_{S_{c,j}} \delta\{u\}^T\{p_c\}dS\right) \\ + \sum_j^n \left(\int_{S_{t,j}} \delta\{u\}^T\{p_t\}dS\right) + \int_\Omega \delta\{u\}^T\{p\}dS\end{aligned} \tag{2}$$

with

$$\Omega = S - \sum_{j=1}^m S_{c,j} - \sum_{j=1}^n S_{t,j} \tag{3}$$

$\{p_c\}$ and $\{p_t\}$ being the force vectors of cohesive and overlapping process zones, respectively and $\{p\}$ the effective load vector acting on the body. Thus, if a finite element approach is used to solve Eq. (1), by means of the shape functions matrix, $[N]$, the matrix $[B]$ containing the derivatives of the shape functions and the elastic matrix $[D]$, it is possible to obtain

$$\left(\sum\int [B]^T[D][B]\mathrm{d}V - \sum\int [C][L][N]\mathrm{d}S - \sum\int [T][L][N]\mathrm{dS}\right)\{\overline{u}\} = \lambda\sum\int \{p\}\mathrm{d}S \tag{4}$$

$[C]$ and $[T]$ being the cohesive and the overlapping matrices set according to Fig. 1b and 1d, respectively; λ a multiplication factor for the external load vector and

$$[L] = \begin{bmatrix} -1 & 1 & 0 & 0 \\ 0 & 0 & -1 & 1 \end{bmatrix} \tag{5}$$

Equation (4) may be transformed as follows

$$([K] - [S_c] - [S_t])\{\overline{u}\} = \lambda\left\{\hat{f}_{ext}\right\} \tag{6}$$

$[S_c]$ and $[S_t]$ being the softening matrix in tension and compression, respectively and $\left\{\hat{f}_{ext}\right\}$, the reference external load vector. The equilibrium Eq. (6) represents an extension of the equilibrium condition initially proposed by Bocca et al. [22] and clearly suggests how in a damaged body, a loss of stability may occur similarly to Euler's buckling [17] since the effective stiffness matrix, $[K_{eff}]$, of the damaged solid is $[K_{eff}] = [K] - [S_c] - [S_t]$. Equation (6) may also be transformed as

$$\{f_{int}\} - \lambda\left\{\hat{f}_{ext}\right\} = \{0\} \tag{7}$$

$\{f_{int}\}$ being the internal force vector.

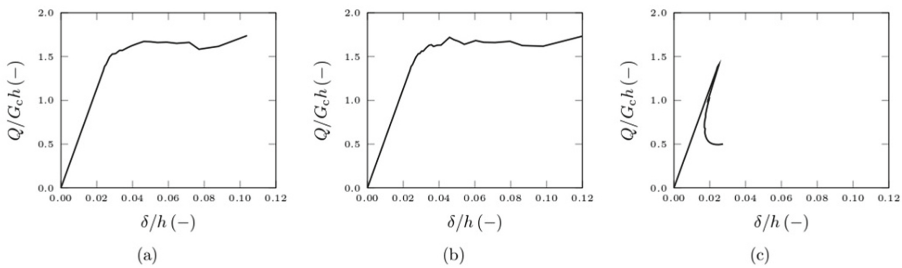

Fig. 3. Scale effects in masonry arches: (a) small scale; (b) medium scale; (c) large scale

Thus, by means of COCM an incremental steady-state analysis may be set according to Eq. (7). On the other hand, if we want to follow snap-back unstable branches in a stable manner, the multiplication factor, λ, must be determined according to a generalized path-following constraint [23] and, more precisely, assuming the crack length increment as controlling loading variable (Crack Length Control scheme). In this framework, at each computation step, it should be ensured that the internal force, f_i, at crack tip i, is equal to the ultimate force f_u set by the cohesive or overlapping constitutive laws (Fig. 1b, d). In this context, by means of Taylor expansion series, the load increment $\delta\lambda$ for each crack tip i between iteration j and $(j+1)$ may be written as

$$\delta\lambda_i^{j+1} = \frac{f_u - f_i^j - \left\{K_{\text{eff},i}\right\}^T [K_{\text{eff}}]^{-1} \left\{r^j\right\}}{\left\{K_{\text{eff},i}\right\}^T [K_{\text{eff}}]^{-1} \left\{\hat{f}_{\text{ext}}\right\}} \tag{8}$$

with $\{r^j\} = \lambda_i^j\{\hat{f}_{\text{ext}}\} - \{f_{\text{int}}^j\}$ and $\left\{K_{\text{eff},i}\right\}$ the i-th row of the effective stiffness matrix. At each computation step, Eq. (8) is solved for each crack tip i and the effective load increment is assumed as

$$\Delta\lambda = \min\left|\sum_j \delta\lambda_i^j\right| \tag{9}$$

In order to simulate the transferring stress capacity along cracks, *zero-thickness interface elements* [24] formed by an upper and a lower layer are employed. These layers have twin nodes sharing same coordinates and for which it is possible to calculate the relative displacement vector, $\{w\}$, as the displacement difference between each twin pairs (see Eq. (5)). Unlike many Fracture Mechanics models [25, 26], in COCM these special finite elements are not inserted in the mesh a priori but, at each computation step, a remeshing algorithm is adopted to modify mesh topology only in the zone ahead the crack tip that reaches the propagation condition. In this context, a reliable simulation of strain localization phenomena occurring in quasi-brittle materials may be performed.

Table 1. Geometrical parameters of the analysed arches

Scale	l (m)	r (m)	h (m)
Small	2.0	0.3	0.1
Medium	20.0	3.0	1.0
Large	200.0	30.0	10.0

3 COCM Applications

3.1 Scale Effects in Masonry Arches

In Fig. 3, numerical curves obtained by means of the application of COCM to masonry arches are presented. Masonry is assumed to have a compression strength $\sigma_c = 30$ MPa, and a tension strength $\sigma_t = 2.6$ MPa, whereas the fracture energy, G_F, and the crushing energy, G_c, are assumed equal to 0.14 and 30 N/mm, respectively. Three different scales have been considered according to a scale factor of 1, 10 and 100 for the arch span, l, the rise, r, and the section depth, h, as reported in Table 1. Each arch is analysed using the same mesh density and in order to have an accaptable computation time, the number of controlled sections along which strain localization phenomena may occur is fixed to 17.

In Figs. 3a and 3b the loading curves obtained for small and medium scales are reported. It is possible to observe that these two arches present a stable behaviour since once the elastic limit is reached, a pseudo-ductile plateau is described. Moreover, a small increase in the bearing capacity of the structure is detected in the post-elastic regime. The ultimate behaviour of these two scales is governed by damage in compression: COCM evidences that crushing takes place in all the 17 controlled sections along the arch span.

On the other hand, the large scale arch reported in Fig. 3c presents a completely unstable behaviour since after the peak load, a catastrophic snap-back is detected. For this scale COCM provides that the ultimate behaviour is mainly governed by cracking processes at the extrados sections close to springings.

3.2 Mosca Bridge Case Study

In this section, COCM will be applied to the investigation of the nonlinear behaviour of the Mosca bridge (Turin, Italy). The bridge was built in the first half of the XIX century and its span is formed by a unique 45 m arch made of local stone. The arch has a rise of 5.5 m and a section depth that varies from 2.0 m (close to abutments) to 1.5 m (close to keystone). The mesh is constructed in COCM following the abovementioned geometrical parameters and, as in the case of the numerical analyses presented in Sect. 3.1, the maximum number of sections along which cracking and crushing damage may occur is fixed to 17.

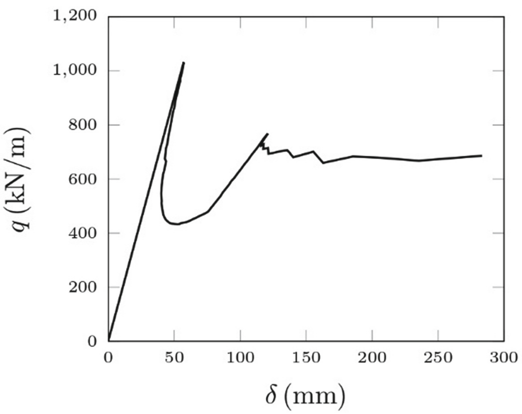

Fig. 4. Load-displacement curve for Mosca bridge

The analysis of the bridge is divided into two parts: in the first part, a parabolic load has been applied to simulate bridge construction phases and, in the second part an incremental analysis by means of COCM as presented in Sect. 2 is performed to investigate its ultimate behaviour.

For the construction phase analysis, it has been assumed a density for the arch granite equal to 27 kN/m^3 and a density of 23 kN/m^3 for the filling. The granite is supposed to have a compression strength $\sigma_c = 50$ MPa, and a tension strength $\sigma_t = 0.3$ MPa, whereas the fracture energy, G_F, and the crushing energy, G_c, are assumed equal to 0.02 and 50 N/mm, respectively. The application of COCM reveals that at the end of bridge construction, cracks are opened at the extrados of springings: these cracks were actually observed during centering removal [27]. On the other hand, with the application of live loads to the structure, these cracks close due to an increase in the compression force. The results of the incremental analysis performed by COCM is reported in Fig. 4 where the uniformly distributed load, q, is plotted against the keystone displacement, δ. It is possible to observe that the bridge has an almost linear behaviour until the peak load. After the peak load, a snap-back branch is detected due to granite crushing at keystone. Then, an increase in the loadbearing capacity is predicted due to cracking phenomena close to keystone and a redistribution of internal stresses: thus, a pseudo-ductile plateau is described until final failure.

4 Conclusions

In this paper, COCM has been integrated in a finite element method to simulate the elastic-plastic-softening loading history of masonry structures taking into account cracking and crushing damage phenomena together with scale effects. The numerical analyses within this paper clearly suggest the existence of a ductile-to-brittle transition in masonry arch bridges by increasing the scale. More precisely, COCM reveals that small scale arches present a pseudo-ductile behaviour similar to reinforced concrete beams: due to diffused damage along the arch span, an effective redistribution of internal stresses may be acknowledged.

The presented theoretical framework may be easily extended to include the effects of a possible FRP reinforcing plate and/or the effects of a dynamic load, providing a complete new approach for the evaluation of curved masonry structures.

References

1. Accornero, F., Lacidogna, G., Carpinteri, A.: Medieval arch bridges in the Lanzo Valleys, Italy: cases studies on incremental structural analysis and fracturing benefit. J. Bridge Eng. (ASCE) **23**(7), 05018005 (2018)
2. Manuello Bertetto, A., Marano, G.C.: Numerical and dimensionless analytical solutions for circular arch optimization. Eng. Struct. **253**, 113360 (2022)
3. Melchiorre, J., Manuello Bertetto, A., Marmo, F., Adriaenssens, S., Marano, G.C.: Differential formulation and numerical solution for elastic arches with variable curvature and tapered cross-sections. Eur. J. Mech.-A/Solids **97**, 104757 (2023)
4. Carpinteri, A., Lacidogna, G., Accornero, F.: Evolution of the fracturing process in masonry arches. J. Struct. Eng. (ASCE) **141**(5), 04014132 (2015)

5. Accornero, F., Lacidogna, G., Carpinteri, A.: Evolutionary fracture analysis of masonry arches: effect of shallowness ratio and size scale. Comptes Rendus Mécanique **344**(9), 623–630 (2016)
6. Heyman, J.: The Stone Skeleton, 1st edn. Cambridge University Press, Cambridge, UK (1995)
7. Lacidogna, G., Accornero, F.: Elastic, plastic, fracture analysis of masonry arches: a multi-span bridge case study. Curved Layered Struct. **5**, 1–9 (2018)
8. Accornero, F., Lacidogna, G.: Safety assessment of masonry arch bridges considering the fracturing benefit. Appl. Sci. **10**(10), 3490 (2020)
9. Carpinteri, A., Corrado, M., Mancini, G., Paggi, M.: Size-scale effects on plastic rotational capacity of reinforced concrete beams. Struct. J. (ACI) **106**(06), 887–896 (2009)
10. Carpinteri, A., Corrado, M., Paggi, M., Mancini, G.: New model for the analysis of size-scale effects on the ductility of reinforced concrete elements in bending. J. Eng. Mech. (ASCE) **135**(3), 221–229 (2009)
11. Carpinteri, A., Corrado, M.: Upper and lower bounds for structural design of RC members with ductile response. Eng. Struct. **33**(12), 3432–3441 (2011)
12. Accornero, F., Cafarelli, R., Carpinteri, A.: Cracking and crushing in prestressed concrete beams. Struct. J. (ACI) **118**(2), 101–109 (2021)
13. Accornero, F., Cafarelli, R., Carpinteri, A.: The cohesive/overlapping crack model for plain and RC beams: scale effects on cracking and crushing failures. Mag. Concr. Res. **74**(9), 433–450 (2022)
14. Accornero, F., Cafarelli, R., Carpinteri, A., Nanni, A.: Scale effects in GFRP-bar reinforced concrete beams. Struct. Concr. **24**(2), 2817–2826 (2023)
15. Carpinteri, A., Accornero, F., Cafarelli, R.: Scale effects in prestressed concrete structures: maximum reinforcement percentage to avoid brittle crushing. Eng. Struct. **225**, 113911 (2022)
16. Hillerborg, A., Modéer, M., Petersson, P.-E.: Analysis of crack formation and crack growth in concrete by means of fracture mechanics and finite elements. Cem. Concr. Res. **6**(6), 773–781 (1976)
17. Carpinteri, A.: Cusp catastrophe interpretation of fracture instability. J. Mech. Phys. Solids **37**(5), 567–582 (1989)
18. Belgin, C.M., Şener, S.: Size effect on failure of overreinforced concrete beams. Eng. Fract. Mech. **75**(8), 2308–2319 (2008)
19. Lourenco, P.B.: Computational strategies for masonry structures, PhD Thesis, Delft University of Technology, Netherlands (1996)
20. Carpinteri, A., Corrado, M., Mancini, G., Paggi, M.: The overlapping crack model for uniaxial and eccentric concrete compression tests. Mag. Concr. Res. **61**(9), 745–757 (2009)
21. Lanczos, C.: The Variational Principles of Mechanics, 4th edn. Dover Publication, New York, USA (1949)
22. Bocca, P., Carpinteri, A., Valente, S.: Mixed mode fracture of concrete. Int. J. Solids Struct. **27**(9), 1139–1153 (1991)
23. Ramm, E.: Strategies for tracing the nonlinear response near limit points. In: Wunderlich, W., Stein, E., Bathe, K.-J. (eds.) Nonlinear Finite Element Analysis in Structural Mechanics, pp. 63–89. Springer Berlin Heidelberg, Berlin, Heidelberg (1981). https://doi.org/10.1007/978-3-642-81589-8_5
24. Goodman, R.E., Taylor, R.L., Brekke, T.L.: A model for the mechanics of jointed rock. J. Soil Mech. Found. Div. (ASCE) **94**(3), 637–659 (1968)
25. Nguyen, V.P.: Discontinuos Galerkin/extrinsic cohesive zone modelling: implementation caveats and applications in computational fracture mechanics. Eng. Fract. Mech. **128**, 37–68 (2014)
26. D'Altri, A.M., et al.: Modeling strategies for the computational analysis of unreinforced masonry structures: review and classification. Arch. Comput. Methods Eng. **27**, 1153–1185 (2020)
27. Castigliano, A.: Théorie de l'Equilibre des Systémes Elastiques et ses Applications. 1st edn. Del Negro, Torino, Italy (1879)